

BASALTIC EXPLOSIVE VOLCANISM IN A TUFF-DOMINATED INTRAPLATE SETTING, SARMIENTO FORMATION (MIDDLE EOCENE- LOWER MIocene), PATAGONIA ARGENTINA

José Matildo PAREDES¹, Ferrán COLOMBO², Nicolás FOIX^{1,3}, José Oscar ALLARD¹, Adriana NILLNI¹ and Mariana ALLO¹

¹Dpto. de Geología, Universidad Nacional de la Patagonia "San Juan Bosco", Ruta Provincial N° 1, Km. 4, (9005) Comodoro Rivadavia, Chubut, Argentina. Email: paredesj@unpata.edu.ar

²Dpto. de Estratigrafía, Paleontología y Geociencias Marinas, Facultad de Geología, Universidad de Barcelona. (08028) Barcelona, España.

³CONICET (Consejo Nacional de Investigaciones Científicas y Técnicas).

Abstract: The Sarmiento Formation (middle Eocene to early Miocene) represents the distal record of the activity of the Andean volcanic arc in central Patagonia, mainly dominated by accumulation and reworking of fine ash in a low-gradient continental setting. Intraplate volcanism takes place in the Golfo San Jorge Basin during the deposition of the Sarmiento Formation, and shallow intrusives and basaltic lava flows occurs. An exposure of basaltic volcaniclastic deposits was analyzed in the proximity of the Cerro Dragón intrusive rocks. These deposits consist of eight volcaniclastic lithofacies, organized in three distinct lithofacies association: volcaniclastic debris flow (lahar), base surge, and scoriaceous breccias of a strombolian-style eruption. Explosive volcanism is evidenced by the fallout of ballistic bombs over base surge and scoriaceous deposits, which produced bedding sags in the plastic lapilli. These deposits constitute the first published record of explosive volcanism (Strombolian) associated to the emplacement of the Oligocene alkaline volcanic rocks in the Golfo San Jorge Basin, generally considered as subintrusive or hypabissal intrusions.

Resumen: La Formación Sarmiento (Eoceno medio a Mioceno inferior) corresponde al registro distal de la actividad del arco volcánico Andino en la Patagonia central, y está caracterizada por la acumulación y retrabajo de ceniza volcánica fina en ambientes continentales de bajo gradiente. Durante la depositación de la Formación Sarmiento tiene lugar un evento volcánico de intraplaca, con intrusivos alcalinos someros y flujos de lavas basálticas. En este estudio se analiza una exposición de depósitos volcanoclásticos basálticos ubicados en adyacencias de las rocas intrusivas del Cerro Dragón. Estos depósitos consisten de ocho litofacies volcánicas, que pueden ser incluidas en tres asociaciones de litofacies: flujos piroclásticos densos (lahar), oleadas piroclásticas y depósitos de brechas de escoria asociados a una erupción estromboliana. La actividad volcánica explosiva se reconoce por la presencia de bombas volcánicas en depósitos de oleadas piroclásticas y de brechas de escoria, que deforman plasticamente los estratos inconsolidados de lapilli. Estos depósitos constituyen el primer registro publicado de volcanismo basáltico explosivo (Estromboliano) asociado al emplazamiento de las rocas volcánicas alcalinas de edad Oligoceno en la cuenca del Golfo San Jorge, consideradas generalmente intrusiones sub-volcánicas o hipabisales.

Keywords: Intraplate volcanism, volcanosedimentary deposits, basaltic bombs, middle Tertiary, Patagonia Argentina

Palabras clave: Volcanismo de intraplaca, depósitos volcanosedimentarios, bombas basálticas, Terciario medio, Patagonia Argentina.

INTRODUCTION

Explosive basaltic volcanism in intraplate settings is usually dominated by low to moderate intensity Hawaiian and Strombolian eruption styles and deposits (Walker, 1993; Parfitt, 2004; Martin and Németh, 2006), and typically construct small monogenetic volcanoes referred as scoria cones, tuff cones and rings, and maars (Vespermann and Schmincke, 2000). The associated pyroclastic deposits are well characterized in young (Pliocene to historical) eruptions (Houghton *et al.*, 1999; Kokelaar, 1986; Cas and Wright, 1987; White, 1991; Parfitt, 2004; Risso *et al.*, 2008, among others). However, due to the low potential of preservation of basaltic volcanoes, there are few studies of older volcaniclastic successions associated to basaltic volcanism (Ayres *et al.*, 1991; Mazzoni, 1994; Németh *et al.*, 2001; Németh and White, 2003; Befus *et al.*, 2008).

The occurrence of several mafic, alkaline intrusive rocks of Cenozoic age takes place in Central Patagonia. These intrusives crop out in the eastern margin of the San Bernardo Fold Belt and have been also identified in seismic surveys in the subsurface of the Golfo San Jorge Basin (Ferello, 1969; Bitschene *et al.*, 1991; Chelotti *et al.*, 1996). Most of these bodies were intruded into shallow crustal levels (< 1 km) and show intrusive contacts to Cretaceous and Paleogene sedimentary rocks. Basaltic lava flows related to these bodies are intercalated into a pyroclastic continental succession known as "Tobas de Sarmiento" or Sarmiento Formation (Simpson, 1940; Feruglio, 1949; Spalletti and Mazzoni, 1977, 1979). The later consist of fine pyroclastic material deposited as distal products of the Andean volcanic arc during \approx 25 m.a. in central Patagonia (Mazzoni, 1985; Bellosi and Madden, 2005) in aeolian and fluvial environments (Mazzoni, 1985; Bellosi *et al.*, 2002; Bellosi, 2005). The Sarmiento Formation contains one of the richest mammal assemblages of Eocene to early Miocene age of South America (Pascual and Odreman Rivas, 1973; Marshall *et al.*, 1977, 1986; Marshall and Pascual, 1978; Legarreta and Uliana, 1994), and three main mammal-ages were identified in the Sarmiento Formation: Casamayorense (early to middle Eocene), Deseadense (late Eocene to Oligocene) and Colhuehuapense (early Miocene). Alkaline lava flows and intrusive rocks of the Sarmiento Formation are related to extensional processes in the retroarc of the Andean volcanic arc (Vietto and Bitschene, 1994; Ardolino *et al.*, 1999; Panza and Franchi, 2002). They have ^{40}K - ^{40}Ar ages variable from 35.4 +/- 0.5 to 21.6 +/- 1.3

ma (Marshall *et al.*, 1986) and could be grouped (Ardolino *et al.*, 1999) into a late Eocene event (35-34 ma) and an Oligocene event (29-25 ma), both included in the Deseadense mammal age (Legarreta and Uliana, 1994).

Miocene volcanic activity continued northwards of the Golfo San Jorge Basin (Meseta Cuadrada-Meseta del Canquel), with the development of an extensive basaltic plateau (Ardolino *et al.*, 1999). Mazzoni (1994) analyzed early Miocene volcanosedimentary deposits at Meseta de Canquel (Scarrit Pocket after Simpson, 1941), north of the Golfo San Jorge Basin, which is until now the unique study of near-vent volcaniclastic deposits in Tertiary rocks of the Golfo San Jorge Basin. Sciuotto *et al.* (2000) provided a detailed review of antecedents, distribution and general considerations of the Sarmiento Formation. A review of occurrence of basaltic rocks of Cenozoic age in central Patagonia was provided by Panza and Franchi (2002).

The aim of this research is to present the results of a detailed lithofacies analysis carried out on a near-vent volcaniclastic succession of the Sarmiento Formation (Deseadense) and discuss their eruptive mechanisms. These deposits are until now the unique mention of subaerial explosive volcanism in Oligocene volcanic rocks of the Golfo San Jorge Basin.

GEOLOGICAL FRAMEWORK

Tectonic Setting

The Golfo San Jorge Basin (Fig. 1a) is a dominantly extensional Basin superimposed on a Precambrian to Palaeozoic continental crust. This basin is broadly E-W orientated and located between the Norpatagónico Massif and Deseado Plateau.

The tectonic evolution of the basin evidences an early Cretaceous synrift stage (Neocomian) that deposited clastic wedges in hemigrabens, currently preserved in the subsurface of the basin. Regional subsidence takes place during the remainder of the Cretaceous, where a continental succession (Chubut Group) about 6000 m thick originates the main hydrocarbon reservoirs of the basin. With the development of the Andean volcanic arc since the uppermost Cretaceous the basin is segmented in three major areas separated by the incipient San Bernardo Fold Belt.

The Golfo San Jorge Basin has been divided according to its structural style (Figari *et al.*, 1999) into five major regions (Fig. 2). Three of these regions are in the eastern part of the Basin (North Flank, Centre of Basin and South Flank), where an extensional style prevails

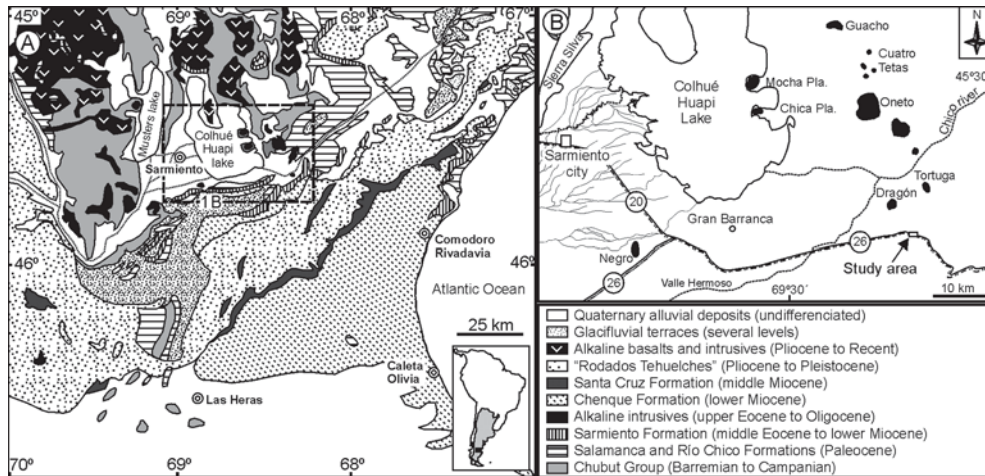


Figure 1. Location maps. a) Geological map of the Golfo San Jorge Basin, b) Location of Tertiary alkaline intrusives (black bodies), main road and localities around the study area.

Figura 1. Mapas de ubicación. a) Mapa geológico de la Cuenca del Golfo San Jorge, b) Ubicación de intrusivos alcalinos Terciarios (cuerpos en negro), rutas principales y localidades en los alrededores del área de estudio.

(Giacosa *et al.*, 2004; Foix *et al.*, 2008). West of this area, is the San Bernardo Fold Belt, which has a NNW-SSE orientation and which rose up mainly during Neogene times (Rodríguez and Littke, 2001). The fifth region, called the Western Sector, is located further west of the Fold Belt and is dominated by extensional structures (Clavijo, 1986), or with little evidence of positive tectonic inversion (Figari *et al.*, 1996). The studied outcrop of this work is located in the eastern margin of the San Bernardo Fold Belt.

Tertiary Stratigraphy

During the uppermost Cretaceous and the Cenozoic, the Golfo San Jorge Basin behaved as a wide tectonic depression with little subsidence. About 900 meters of sediments were preserved (Fig. 3), with alternation of transgressive episodes and continental sedimentation in the continental margin. All the units have pyroclastic components derived from the intermittent magmatic activity of the Andean volcanic arc. Over more than 6000 m of continental sediments of the Chubut Group (Barremian to Campanian) an Atlantic marine transgression occurred in the Golfo San Jorge basin. The preserved rocks are known as the Salamanca Formation (Lesta and Ferello, 1972) and represent platform and estuarine environments formed during a Maastrichtian to Danian time span.

From the upper Danian to the Thanetian, transitional and shallow marine environments (Feruglio, 1949) evolved to high-sinuosity fluvial deposits with

paleosols known as the Río Chico Formation (Marshall *et al.*, 1981). Towards the interior of the Basin, facies of this unit are laterally equivalents to pyroclastic events (Tobas de Koluel Kaire) of the Sarmiento Formation (Legarreta *et al.*, 1990).

From early-middle Eocene to early Miocene times, extensive tuff strata that belong to the Sarmiento Formation were deposited in a low-gradient, continental setting. Their deposits are less than 200 m thick, indicating low subsidence rate and scarce sediment supply to the basin.

The Chenque Formation (Bellosi, 1990) corresponds to an Atlantic transgression, early Miocene in age. This unit is in part coeval with the upper Member of the Sarmiento Formation (Cohuehuapense), deposited in a deep incised valley (Bellosi *et al.*, 2002). These marine sediments grade to high-sinuosity fluvial and aeolian deposits, known as the Santa Cruz Formation or "Santacruciano" (Feruglio, 1949; Lesta *et al.*, 1980), which has been assigned, according to radimetric ages, to the Burdigalian-Langhian interval (Feagle *et al.*, 1995).

Since middle Miocene times the Golfo San Jorge Basin has been subjected to an erosive regime related to the elevation of the Andean volcanic arc and to an overall fall in the sea level. The post-Miocene deposits are scarcely represented, with the remarkable exception of gravel beds known as the "Rodados Tehuelches", which constitute high-energy fluvial systems associated with the melting of extensive glaciations in Pliocene and Pleistocene times.

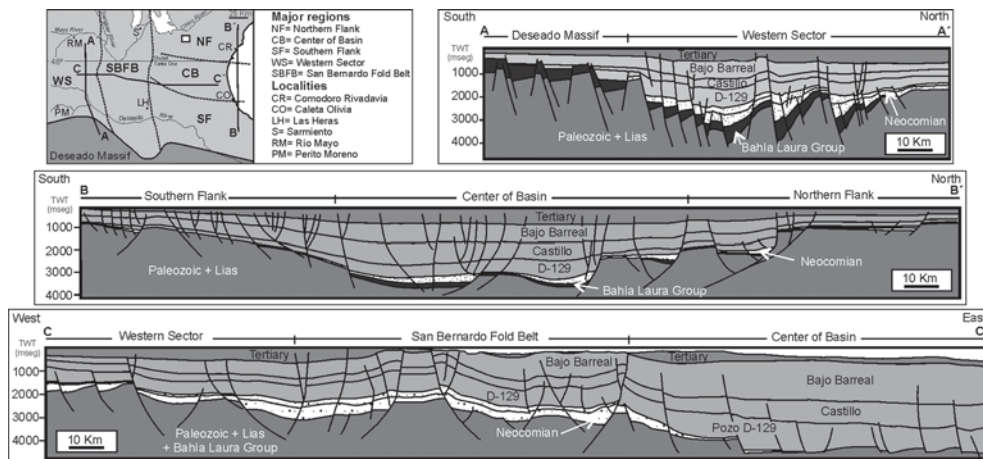


Figure 2. Major structural subdivisions and regional seismic sections in the Golfo San Jorge basin. Extensional features dominate the Eastern Sector of the Basin (B-B' seismic line) and the Western Sector (A-A' seismic line), where subtle evidence of positive inversion is also observed. The E-W section (C-C' seismic section) shows the San Bernardo Fold Belt in the centre and the increases in thickness of the Chubut Group to the east (after Figari *et al.*, 1999; Hechem and Strelkov, 2002).

Figura 2. Principales subdivisiones estructurales y secciones sísmicas regionales en la Cuenca del Golfo San Jorge. Los rasgos extensionales predominan en el Sector Oriental de la cuenca (línea sísmica B-B') y en el Sector Occidental (línea sísmica A-A'), donde se observa alguna evidencia de inversión positiva. La sección E-O (línea sísmica C-C') muestra la Faja Plegada de San Bernardo en el centro y el incremento de espesor del Grupo Chubut hacia el este (tomado de Figari *et al.*, 1999; Hechem and Strelkov, 2002).

METHODOLOGY AND TERMINOLOGY

This study focuses on a road-cut outcrop located in the km. 70 of the State Road N° 26 that joins Comodoro Rivadavia and Sarmiento cities, immediately eastward of Baltazar Restaurant ($S\ 45^{\circ} 43' 30''$, $W\ 68^{\circ} 19' 12''$). This exposure is isolated in relation to the remainder of the Sarmiento Formation, and is 2 km southeastward of the intrusive rocks of the Cerro Dragón (Fig. 1b).

Three bed-by-bed stratigraphical sections were constructed along a 160 m long exposure (Fig. 4), which is inclined 7° to 205° . Data collected during outcrop examination includes lithology, stratal thickness, texture, mean and maximum grain size, mechanical sedimentary structures, measurement of size and axis of basaltic bombs and identification and characterization of faults. Microscopic features including grain composition and textures were obtained from 12 polished thin sections. Grain size distribution of base surge and lahar deposits were realized. Volcaniclastic rocks are described according to grain size (ash, < 2 mm, lapilli, 2-64 mm, and block (lithic) or bomb (juvenile), > 64 mm). When necessary, bed thickness follows Ingram (1954) classification: laminated, < 1 cm; very thinly bedded, 1-3 cm; thinly bedded, 3-10 cm; medium bedded, 10-30 cm; thickly bedded, 30-100 cm; very thickly bedded, > 1 m. The descriptive terms bombs and blocks

are used according to Macdonald (1972) and Fisher and Schmincke (1984).

SEDIMENTOLOGY

The volcaniclastic succession has been subdivided into eight volcaniclastic lithofacies, and description and interpretation of transport conditions, depositional processes and origin are summarized in Table I. The lithofacies can be organized in three main lithofacies associations: matrix-supported debris flow (lahar), base surge, and clast-supported, scoriaceous breccia. Each lithofacies association is defined on the basis of spatial association, contact relationship and inferred genetic affinities. Details of the lithofacies are presented in Figures 5 to 8.

Lithofacies Association 1: Volcaniclastic debris-flow (lahar)

Description: A conspicuous bed in the studied exposure is characterized by irregular to non-erosional base, poor sorting, absence of vertical grading (locally inverse grading at the base) and a general lack of internal organization (Fig. 4). It is mostly composed by matrix-supported, faceted to low-rounded basaltic blocks (lithofacies LF1) with variable vesicular content, and a matrix composed of basaltic lapilli (Fig. 5a). Some blocks have vertical elongation of the a-axis. The deposit is 1.3 to 1.5 m thick and has a matrix content

Lithofacies name	Characteristics	Interpretation	Lithofacies association
LF1. Disorganized matrix-supported lapilli and blocks	Sharp, non-erosional base. No grading or organized fabric. Random alignment of angular or poorly-rounded, basaltic clasts. In places bed consist of a single basaltic block. Matrix (>20-35% common) is fine lapilli and minor ash. Scarce white, siliceous concretions. Bed thickness varies from 0.8 to 1.5 m. Grain sizes to 2-3 cm, maximum clast size: 130 cm.	<i>In</i> mass deposition from volcanic, cohesionless debris flow	<i>Lahar</i>
LF2. Plane-parallel stratified, clast-supported lapilli	Sharp or gradational base. Inversely graded or ungraded strata. Amalgamated thin beds with diffuse contacts. Some massive, medium sandstone layers pinch out as lenses. Massive or with horizontal stratification. Poorly-rounded clasts, moderate selection in grain sizes. Rare outsized clasts until 8 cm. Matrix is coarse ash. Bed thickness ranges from 0.4 to 0.8 m.	Hyperconcentrated flood flow; migration of low-relief amplitude and high-wavelength dunes.	Base surge
LF3: Lapilli with antidune bedding	Plane base. Ungraded or normally graded beds. Moderate to good selection in grain sizes. Low angle cross-sets up to 0.15 m thick and 1.5-2.0 m long. Foresets dip 8-12° forward and 6-8° backward.	Migration of low-relief bedforms, formed by tractional currents under upper-flow regime conditions.	
LF4: Cross-bedded lapilli and coarse ash	Scoured base and lenticular geometry. Cut and fill structures. Strata show moderate-to-good selection of grain sizes and normal gradation of grain sizes. Contain low angle, sigmoidal cross-bedding and trough cross bedding. Cross-sets are up to 0.4 m thick and a few meters long. Locally contain disturbed bedding.	Migration of subaqueous dunes by dilute flows under lower-flow regime conditions.	
LF5: Faceted to nearly circular basaltic blocks	Low-rounded to faceted fragments of low-vesiculated, hardly consolidated, basaltic scoria. Plastic, asymmetric deformation of the underlying substrate is a typical feature of this facies. Some bombs are elongate to nearly circular in cross section, show concentric layers of different consolidation. Size ranges from 15 to 36 cm.	Ballistic fallout of volcanic bombs	Disrupted base surge or scoriaceous breccia.
LF6: Matrix supported lapilli	Plane base, tabular to lensoidal geometry. Crude bedding or massive aspect. Ungraded strata, moderate to poor selection of grain sizes. Dispersed clasts of poorly-rounded fine gravels. Occasional white, siliceous concretions. Thickness ranges from 0.05 m to 0.4 m.	Hiperconcentrated flood-flow; rapid deposition from suspension	Base surge
LF7: Volcanic ash	Plane base and lenticular geometry. Thin (< 15 cm thick) strata, massive to parallel laminated. Preserved in shallow depressions.	Suspension fallout. Maximum fragmentation of magma	
LF8: Unsorted, clast-supported breccia	Unsorted basaltic blocks and lapilli, fragments of scoria faceted to irregular with variable vesicle content. Clast-supported fabric with minor interstitial ash (< 10%). Basaltic fragments represent >90% of the deposit. Occasional basaltic lithics (some up to 1m in size) containing xenolithes of olivine and pyroxene. Rare blocks of tuffs, thermally altered.	Ballistic fallout of pyroclasts proximal to the source vent.	Strombolian-style eruption

Table I. Recognized lithofacies of the volcanioclastic deposits of the Sarmiento Formation, 2 km southeastward of Cerro Dragón alkaline bodies.
Tabla I. Litofacies reconocidas en los depósitos volcanioclasticos de la Formación Sarmiento, 2 km al sudeste de los cuerpos alcalinos del Cerro Dragón.

variable from 20 % to 35 % of the surface of the exposure. It shows very poor selection and polymodal distribution of grain sizes, with main subpopulations at -6 and -3 ϕ , and a minor subpopulation at -1 to 0 ϕ (Fig. 10). The bed comprises basaltic lithic fragments up to 1 m in diameter, although most of the boulders of dense rocks are less 0.5 m in averaged diameter. Many blocks have dense appearance and show very low vesicle content (Fig. 5c). Other lithic fragments show a slightly vesiculated interior and a non-vesicular external crust, where vesicles are circular or elongated with their a-axis parallel to the external surface (Fig. 5b,d). A low proportion of blocks are highly vesicu-

lated, they are deeply weathered to iron oxides.

Interpretation: The above characteristics suggest transportation and deposition from a highly concentrated flow without formation of traction-related structures or sorting of grain sizes by attenuation of turbulence due to high-concentration of particles into the flow (Lowe, 1982; Postma, 1986; Coussot and Meunier, 1996). Laminar flow conditions are inferred due to the heterogeneity of grain sizes and erratic to vertical orientation of lithic fragments. Inverse grading may indicate the presence of dispersive pressure, due to grain-grain interactions (Arguden and Rodolfo, 1990). In spite of their monolithologic character, the source of the com-

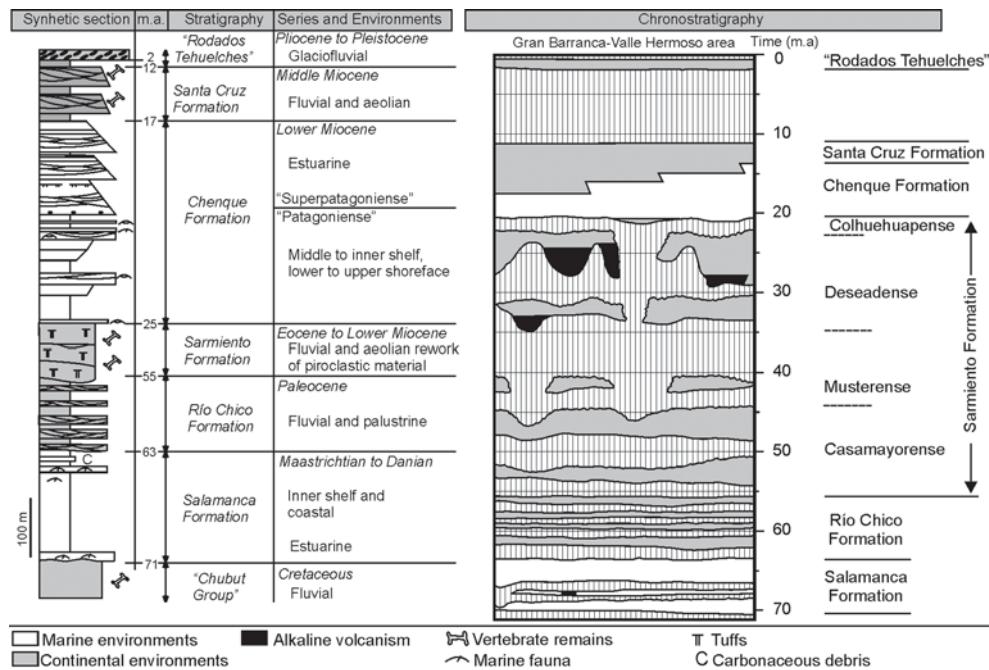


Figure 3. Tertiary stratigraphy of the Golfo San Jorge Basin. On the right the chronostratigraphy of the Gran Barranca - Valle Hermoso area is simplified after Legarreta and Uliana (1994), with indication of the «mammal ages» of the Sarmiento Formation. Basaltic lava flows of the area are emplaced in «Deseadense» rocks.

Figura 3. Estratigrafía Terciaria de la cuenca del Golfo San Jorge. A la derecha la cronoestratigrafía del área Gran Barranca – Valle Hermoso, simplificada de Legarreta y Uliana (1994), con indicación de las «edades mamífero» de la Formación Sarmiento. Los flujos basálticos del área están emplazados en rocas del «Deseadense».

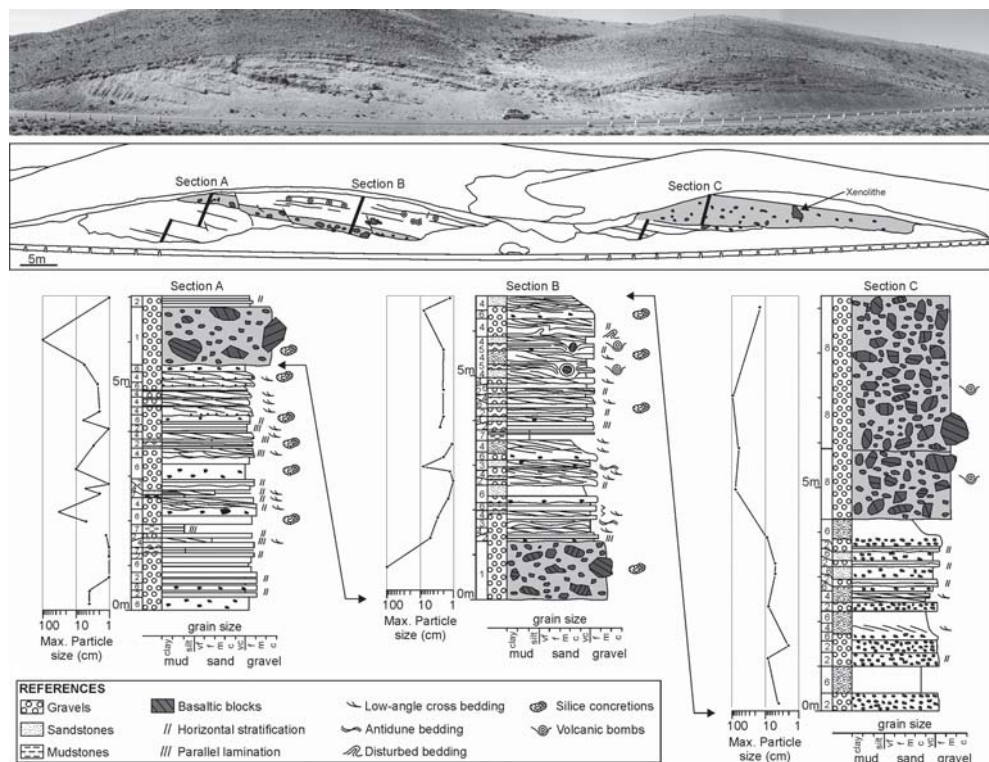


Figure 4. Outcrop view and measured stratigraphic sections. Lithofacies are indicated left of the profiles. Maximum particle size = mean of 10 largest clasts per bed at station.

Figura 4. Vista de afloramiento y secciones estratigráficas realizadas. Las litofacies se indican a la izquierda de cada sección. Tamaño máximo de partícula = promedio de los diez clastos de mayor tamaño del estrato en cada punto de medición.

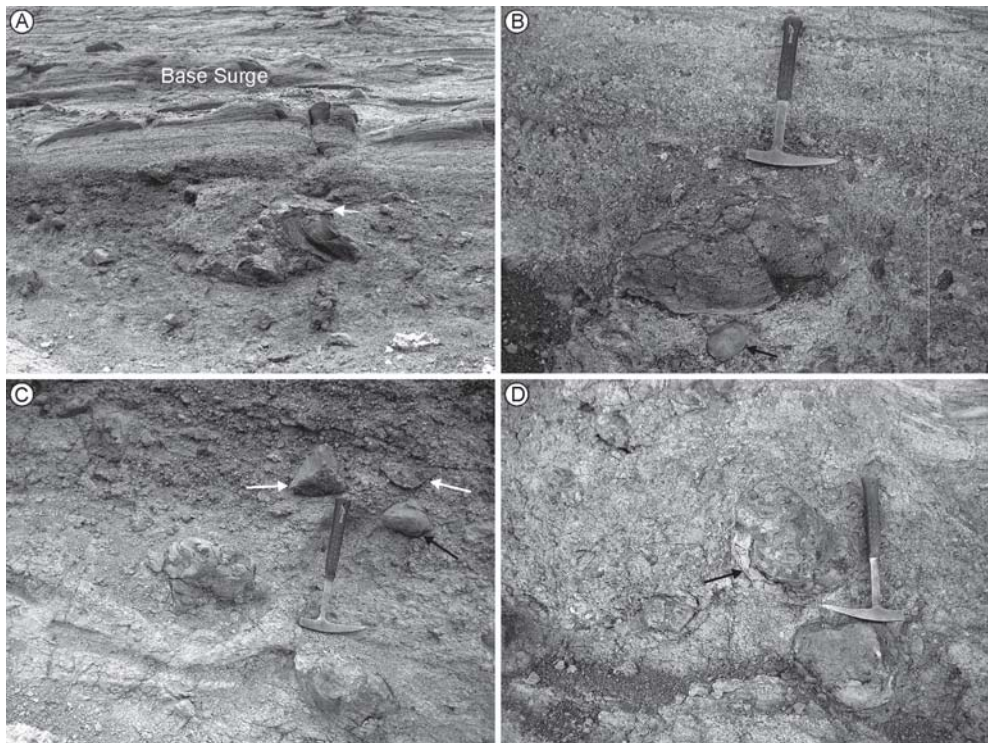


Figure 5. Details of volcaniclastic debris flow (lahar) lithofacies association. a) Unsorted lapilli and blocks (LF1) with dense, angular basaltic fragments. White arrow points to a pen 13 cm long. b) Variable-vesiculated basaltic fragment incorporated into the debris flow. Note the increase in the degree of vesiculation from the crust to the centre of the fragment. Below (arrow) a dense, rounded, basaltic lithic fragment. Hammer is 0.3 m long. c) Faceted (white arrows) and rounded (black arrows) lithic fragments in the unsorted debris flow. In places, deformation of the underlying base surge is produced below of the largest lithic fragments. d) Faceted and rounded clast in a matrix of fine lapilli. Some fragments (arrow) show radial cracks on the crust and exfoliations in concentrical layers due to cooling of the material.

Figura 5. Detalles de la asociación de litofacies de flujo denso volcanoclástico (lahar). A) Lapilli y bloques sin selección con fragmentos basálticos angulares y densos. La flecha blanca apunta a un lápiz de 13 cm de largo. b) Fragmento de basalto con vesicularidad variable incorporado dentro del flujo. Notar el incremento en el grado de vesiculación desde la corteza hacia el centro del fragmento. Por debajo (flecha) un fragmento denso, basáltico, redondeado. El martillo mide 0.3 m de largo. c) Fragmentos líticos facetados (flecha blanca) y redondeados (flecha negra) en el flujo denso sin selección. En sectores se produce deformación de las oleadas piroclásticas subyacentes por debajo de los fragmentos líticos de mayor tamaño. d) Clastos facetados y redondeados en una matriz de lapilli fino. Algunos fragmentos (flecha) muestran grietas radiales en la corteza y exfoliaciones en capas concéntricas debido a enfriamiento del material.

ponents of the flow is variable. Dense basaltic lithics were incorporated into the flow after consolidation, but basaltic fragments with high proportion of vesicles in the interior and dense external crust imply incorporation of partly solidified fragments (e.g. bombs, see below) to the flow (Miyabuchi *et al.*, 2006). There is no macroscopical evidence that could point to decide if the volcanic debris flow is directly related to a volcanic event or if it represents the reworking of previously deposited volcanic detritus (e.g. degassing structures, thermal alteration of surrounding rocks). However, monolithologic varieties are likely to be derived directly by eruption (Fisher and Schmincke, 1984).

Lithofacies Association 2: Base Surge

Description: Two base-surge deposits occur at the section (Fig. 4). The basal contact of the lower occurrence is not exposed, but the lower contact of the upper base-surge deposit is sharp or locally gradational in a short vertical distance up to lahar deposits (Fig. 6b). These deposits are characterized by fine conglomerate containing a variety of primary sedimentary structures, such as plane-parallel stratification and lamination (lithofacies LF2), antidune cross-bedding (lithofacies LF3) and low-angle, through and sigmoidal cross-bedding (lithofacies LF4). Some thinly-to-medium bedded strata have crude bedding and have poor selection of grain sizes (lithofacies LF6), they also were found in the lower part of strata that belong to lithofacies LF4. Well sorted lenses of laminated ash (lithofacies LF7)

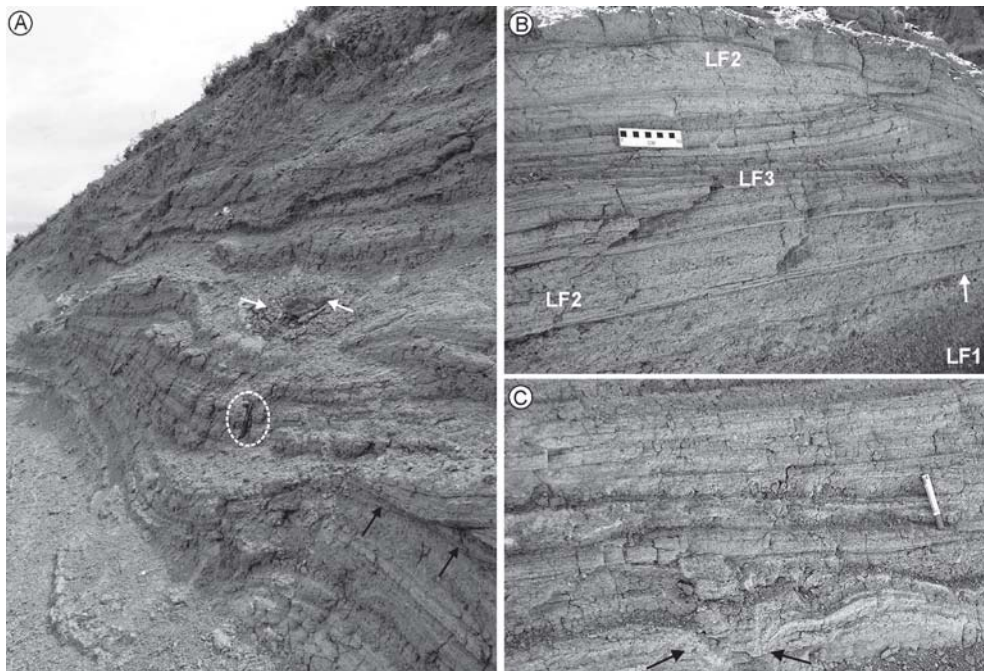


Figure 6. Details of Base Surge lithofacies association, a) Low-relief, high-wavelength dunes with aggradational occurrence of plane-laminated lapilli (LF2). Scour surfaces between bedforms are shown in the lower right corner (black arrow). In the center of the picture a basaltic bomb (indicated by arrows) produces bedding sags in the lapilli. Pen (encircled) is 13 cm long. b) Sharp contact (arrow) between the lahar deposit (LF1) and plane-stratified lapilli (LF2). Lapilli with antidune bedding (LF3) are displayed in the upper part of the picture. Flow is from left to right. Scale graduated in centimeters. c) Migration of low relief, large wavelength dunes with subtle variations in thickness of laminae or strata. Local deformation of strata (arrows) is produced by fallout of basaltic bombs.

Figura 6. Detalle de la asociación de litofacies de oleadas piroclásticas, a) Dunas de bajo relieve y alta longitud de onda, estratos de lapilli con laminación paralela (LF2) presentan un arreglo agradacional. Abajo a la derecha se observan superficies de corte entre formas de fondo. En el centro de la figura se observa una bomba basáltica (indicada con flechas) que produce deformación plástica en el lapilli. El lápiz indicado con un círculo mide 13 cm de largo. b) Contacto neto (flecha) entre depósitos de lahar (LF1) y lapilli con estratificación paralela (LF2). En la parte central y superior de la figura se observa lapilli con estratificación de antiduna (LF3). El flujo es de izquierda a derecha. Escala graduada en centímetros. c) Migración de dunas de bajo relieve y gran longitud de onda, con sutiles variaciones en el espesor de las láminas o los estratos. La caída de bombas basálticas produce deformación local de los estratos (flechas).

were preserved in local depressions. Individual beds range in thickness from 0.3 to 0.8 m, they frequently show a slightly fining-upward trend and present moderate selection of grain sizes. The superposition of surge events frequently occurs on a basal erosional surface, infilled by base-surge deposits with channelized appearance (Fig. 6a). The overall geometry of this lithofacies association is tabular, but individual strata show important thickness variations on local topographic irregularities or due to erosion by superimposed channelized strata. Disturbed bedding is a typical feature of this lithofacies association. Volcanic bombs are common (Figs. 6c and 8).

Thin sections reveal that 65-80% of the matrix is composed of volcanic glass with variable degree of alteration to argillaceous components (Fig. 9b). Interstitial glass is preserved as a colorless to pale-yellow va-

riety, with index less than balsam. Lithics are represented by dark grey porphyritic basalts (Fig. 9a) with scarce (~10-15%) phenocrysts of plagioclase, clinopyroxene, biotite and quartz. Their ferromagnesian components are frequently altered to a mixture of iron-oxides with reddish coloration.

Grain size analysis of the lower base surge deposit (Fig. 10) evidences a bimodal distribution, with major subpopulations at 0 and 2 ϕ . The upper base surge shows a polymodal distribution of grain sizes, with major subpopulations at -1, -3 and -5 ϕ , and higher proportion of finer lithologies.

Interpretation: The abundance of unidirectional current structures and volcanic composition of this lithofacies association is evidence of a dilute, laterally directed pyroclastic density current (base surge) (Fisher and Schmincke, 1984; Cas and Wright, 1987). Vertical

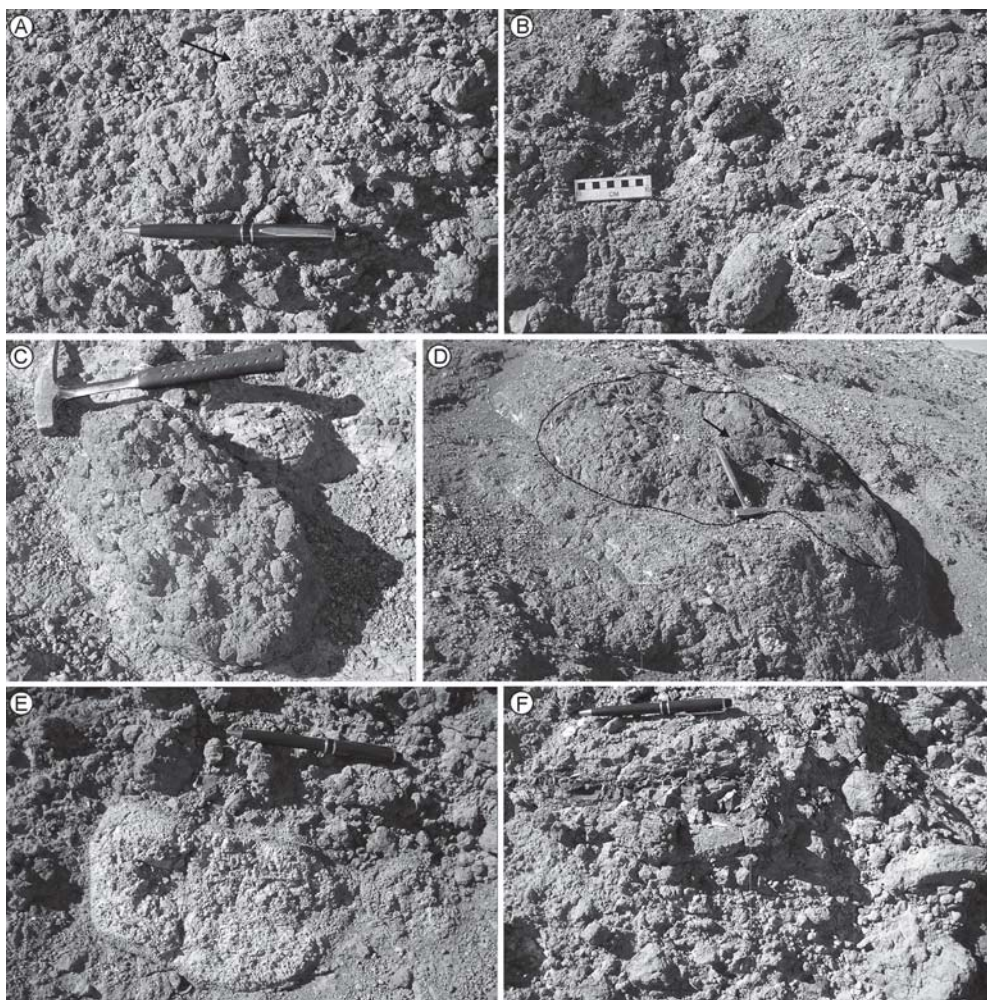


Figure 7. Scoriaceous breccia lithofacies association. a) Typical clast-supported texture of the basaltic breccias (LF8). Note the irregular shape of most of the fragments, and occasional occurrence of highly-vesiculated lithics (arrow). Pen is 13 cm long. b) Faceted to rounded lithic fragments. The encircled fragment has radial cracks due to thermal contraction. c) Agglutinated, basaltic lithic fragment. Hammer is 0.3 m long. d) A dense lithic fragment 1.3 m in size, which contains olivine and pyroxene xenoliths (pointed by the arrows). e) Rounded lithic fragment of tuff incorporated to the breccia. It is suggested that the fragments was rounded by abrasion into the vent. f) Thermally altered lithic fragment of tuff, coated with vesiculated basalts. Note the cracks of the tuff fragment, due to heating and later cooling of the ejected material.

Figura 7. Asociación de litofacies de brechas de escoria. a) Textura clasto soportada típica de las brechas basálticas (LF8). Notar la forma irregular de la mayoría de los fragmentos, con presencia ocasional de líticos altamente vesiculados (flecha). El lápiz mide 13 cm de largo. b) Fragmentos líticos facetados a redondeados. El fragmento dentro del círculo tiene fracturas radiales, producidas por contracción térmica. c) Fragmento lítico basáltico aglutinado. El martillo mide 0.3 m de largo. d) Fragmento lítico denso de 1.3 m de diámetro, que contiene xenolitos de olivino y piroxeno (indicado por las flechas). e) Fragmento lítico de tobas redondeadas incorporado a la brecha. Se interpreta que el fragmento fué redondeado por abrasión dentro del conducto de emisión del cráter. F) Fragmento lítico de toba, alterado térmicamente y recubierto por basaltos vesiculados. Notar las fracturas del fragmento de toba, debidas al calentamiento y posterior enfriamiento del material eyectado.

and lateral relations of identified lithofacies indicate fully turbulent conditions, and transportation in upper and lower flow-regime conditions (Sohn and Chough, 1989). Attenuation of turbulence is due to temporal-spatial variations in the proportion of clasts in movement into the flow, where preservation of ungraded,

massive strata took place (Smith, 1987). Lenses of laminated ash strata are associated to fallout from a contemporary ash cloud (Walker, 1984). The occurrence of surges on top of matrix supported deposits (lahar) with preservation of antidune bedding up to beds containing plane stratification is evidence of flow-trans-

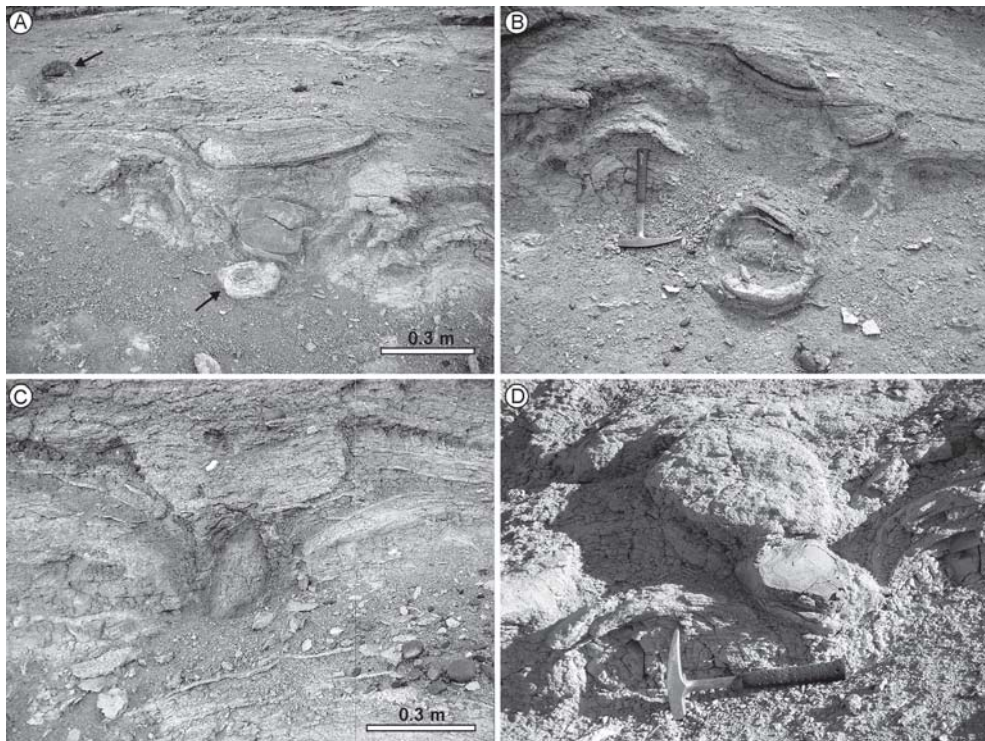


Figure 8. Volcanic bombs. A) Bombs (arrows) and associated bedding sags in the lapilli-sized base surge deposits. In the center of the picture a faceted, dense lithic fragment is incorporated into the sag. Note the lensoidal, near-symmetrical infill of the bomb sag. b) Circular bomb with external crust and layers of different consolidation. Bedding sag is almost symmetrical and 0.5 m in depth. Note the small-scale normal fault in the upper right part of the picture. c) Fusiform volcanic bomb of poorly-consolidated basalts. d) Volcanic bomb of previously consolidated, dense, basaltic material.

Figura 8. Bombas volcánicas. a) Bombas (flechas) y deformación plástica de los depósitos de oleadas piroclásticas, formados por estratos tamaño lapilli. En el centro de la figura un fragmento lítico denso, facetado, ha sido incorporado en la depresión resultante. b) Bomba circular con corteza exterior y capas de diferente consolidación. La deformación del lapilli subyacente es casi simétrica y de 0.5 m de profundidad. Notar la falla normal de pequeña escala en el borde superior derecho de la foto. c) Bomba fusiforme de basaltos pobemente consolidados. d) Bomba volcánica basáltica de material denso, previamente consolidado.

formation processes upward (Fisher, 1979) involving dilution of the head flow and development of upper-and-lower flow regime conditions (Vazquez and Ort, 2006). Abundance of cut-and-fill structures and channeling are related to several large turbulent eddies or pyroclastic surges *sensu stricto* that occur as a series of pulses. Convolute bedding is associated to soft-sediment deformation of strata before consolidation (Pettijohn and Potter, 1964).

The low index of refraction of the glass indicates a glass high in silica. High proportion of silica in volcanic glass derived from basaltic lavas has been related to alteration processes during volcanic degassing and/or explosions (Wohletz, 1983; Spadaro *et al.*, 2002), but due to the pyroclastic nature of the Cretaceous-Paleocene substrate it is possible that silica-rich glass could be partly derived from the fusion of previous

sedimentary rocks.

The variable proportion of ash matrix in strata containing a variety of primary current structures and the bimodal-to-polimodal distribution of grain sizes of Lower and Upper surge deposits suggest that the medium of transportation was a mixture with variable content in gas and steam (Walker, 1984). Abundance of ash matrix in tractionally deposited successions with variable grain size selection is inconsistent with a water-supported system, due to the winnowing and removal of fines produced by that agent (Bull and Cas, 2000).

Lithofacies Association 3: Clast-supported, scoriaceous breccia

Description: These deposits conform the top of the exposure, and consist of 2 amalgamated very thick beds (> 2.2 m each) of loosely packed, unstratified, scoria-

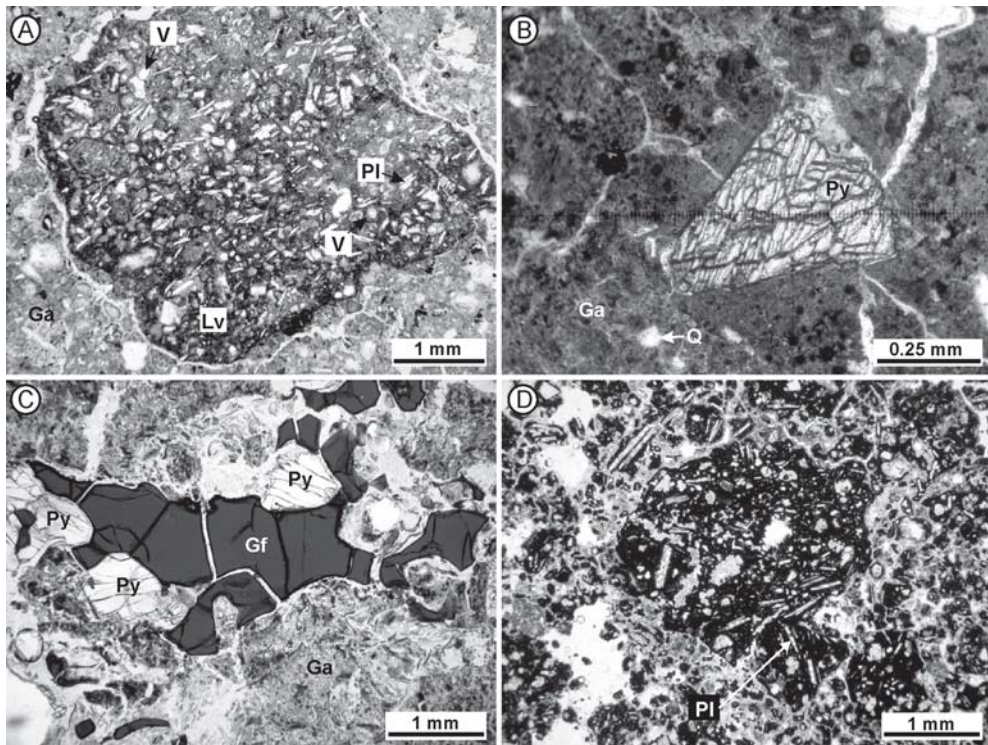


Figure 9. Photomicrograph (parallel nicols) of volcaniclastic lithofacies of the Sarmiento Formation. a) Photomicrograph of lapilli-sized matrix of base surge deposits (lithofacies LF4). Rounded, basaltic-lithic grain (Lv) with porphyritic texture contains oriented plagioclase crystals (Pl) and small vesicles (V). b) Photomicrograph of base surge deposits (lithofacies LF 2). In the center, a basal section of clinopyroxen crystal is rounded by strongly altered volcanic glass (Ga). c) Photomicrograph of the volcanic bomb of Fig. 8e (lithofacies LF 5). In the center, dark fresh volcanic glass (Gf) and prismatic sections of clinopyroxen crystals (Py), both rounded by strongly altered volcanic glass (Ga). d) Photomicrograph of lapilli-sized matrix of the scoriaceous breccia (LF 8). Basaltic lithic in the center of the picture show elongate, plagioclase crystals (Pl) with altered margins. These are rounded by a pervasive, opaque matrix with abundant content in iron oxides.

Figura 9. Microfotografías (nicoles paralelos) de litofacies volcanoclásticas de la Formación Sarmiento. a) Microfotografía de la matriz tamaño lapilli de los depósitos de oleadas piroclásticas (LF4). Líticos redondeados de basalto (Lv) con textura porfirítica contienen cristales orientados de plagioclasa (Pl) y vesículas pequeñas (V). b) Microfotografía de depósitos de oleadas piroclásticas (lithofacies LF2). En el centro, una sección basal de un cristal de clinopiroxeno está rodeada por vidrio volcánico muy alterado. c) Microfotografía de la bomba volcánica de la Fig. 8e (litofacies LF5). En el centro, vidrio volcánico oscuro y fresco (Gf) y secciones prismáticas cristales de clinopiroxeno (Py), ambos rodeados por vidrio volcánico muy alterado (Ga). d) Microfotografía de la matriz tamaño lapilli de las brechas de escoria (lithofacies LF8). El lítico basáltico en el centro de la foto muestra cristales alongados de plagioclasa (Pl) con bordes alterados. Estos están rodeados por una matriz opaca conteniendo abundantes óxidos de hierro.

ceous fragments (lithofacies LF8). The deposit is very coarse grained (> 64 mm), shows a clast-supported texture without orientation of blocks, and most of the components are angular to irregular in shape (Fig. 7a). Up to 90 % of the tephra are basaltic fragments with occasional basaltic lithics up to 1 m in diameter (Fig. 7d). There is a large variety of basaltic lithic fragments: 1) Irregularly shaped, highly-vesiculated basaltic fragments with high proportion of small vesicles (3-4 mm in diameter) and planar margins (Fig. 7a); 2) Elongated to rounded blocks of slightly vesiculated basalts, which show a characteristic weathering pattern of concentric

exfoliations and radial fractures on the surface (Fig. 7b); 3) Outsized pyroclasts (> 50 cm of length in a-axis) of dense basaltic fragments with their a-axis in near-horizontal position, some containing xenoliths of peridotite and clinopyroxene, and 4) Elongated, spindle or flattened basaltic fragments, slightly vesiculated and with discoidal shapes. Some of the largest observed blocks are aggregates of small-sized lapilli (or blocks) of the above mentioned varieties (Fig. 7c).

Accidental lithics are relatively uncommon, and two distinctive varieties were identified: 1) Elongated fragments of thermally-altered tuffs that are concentrically

coated by slightly vesiculated basalts, the later containing radial, superficial cracks (Fig. 7f), and 2) Sub-rounded to rounded, pale red to yellow, thermally altered tuffs (Fig. 7e).

Matrix comprises coarse ash to lapilli-sized clasts, and represents less than 10% of the exposure. Thin section of the matrix that surround volcanic blocks reveals an increase in content and size of the plagioclase crystals (up to 30 % and 2 mm), which are andesine with intersertal groundmass. The volcanic lithics are porphyritic, subangular and of basaltic composition. Mafic components are strongly altered to iron oxides and occur as pseudomorphs (Fig. 9d).

Interpretation: The lack of primary current structures nor vertical grading, massive appearance, very low proportion of interstitial matrix and coarse grain size of the deposit are attributed to deposition by fall-out of different varieties of juvenile and accidental lithics during a Strombolian-style eruption (Fisher and Schmincke, 1984). The variety of features preserved in basaltic blocks evidence different sources for the volcanic detritus. Dense basaltic lithics are likely to the sourced from crater walls or from solidified edges of the conduit (Cas and Wright, 1987). Large blocks containing volcanic xenoliths imply a deep source for some basaltic fragments. On the other hand, the vesicular varieties could have a great number of origins. Elongated and spindle shaped varieties are interpreted as bombs ejected in a plastic state from the lava source. Alternatively, rounding of vesiculated pyroclastics could be due to attrition as they bounded down the side of the cone or vent (Francis, 1973). Slightly vesiculated basaltic lithics with radial cracks reflect thermal contraction during cooling of pyroclastics (Cole *et al.*, 2005). Rare accidental fragments are represented by thermally altered tuffs that were ejected from the source coated with basalt (cored bombs *sensu* Brady and Webb, 1943). Rounded lithics of tuffs were produced in-vent by abrasion during eruption (Cas and Wright, 1987). The low proportion of ash-sized particles is attributed to low volatile content in the basaltic magma, which prevents the development of a large eruptive plume; addition of phreatic or phretomagmatic water could be invoked for the production of ash-sized particles (Cas and Wright, 1987).

Volcanic Bombs

Additionally to the above mentioned bombs preserved in the scoriaceous breccia, the most spectacular evidences of explosive volcanism are preserved in the

base surge lithofacies association. A large number of basaltic bombs were incorporated in the base-surge association in a level about 1.7 m thick. The bombs consist of a core composed of two main lithological types: a) fine-grained, dense or poorly vesicular, sub-angular to faceted basaltic rocks, which represent non-juvenile ejects (Fig. 8d), and b) low consolidated, elongated to spherical basaltic blocks containing large crystals of light-green olivine, clinopyroxene and volcanic glass (Fig. 8c). The later bombs present around the core concentric layers of consolidated, aggregated lapilli (Fig. 8b) or could show dense margins and a more vesiculated interior. Thin sections (Fig. 9c) reveal that volcanic glass is the dominant component of these bombs (up to 80 %), with minor content in clinopyroxene and olivine crystals (~20 %). The most common glass variety is a colorless, pale yellow glass with index less than balsam, commonly altered to argillaceous material; a second variety of glass consist of unaltered, darker to opaque glass with index of refraction greater than balsam. Most bombs are fusiform to spherical in shape, their sizes ranges from 10 to 36 cm in a-axis length (or diameter). The orientation of four inclined a-axis of the bombs indicate a source-vent located NNW of the studied section (340° , standard deviation: 14°), where the Cerro Dragón alkaline bodies are exposed.

The fall of ballistic ejects in the still plastic base-surge beds produced bomb sags, a typical deformation of the substrate which is strong evidence of contemporaneous explosive, subaerial volcanism (Fisher and Schmincke, 1984). In the studied section, bomb sags are up to 0.5 m thick, their size increase with the mass of the ejected bomb (Fig. 8a,b), but it is also related to their ejection angle and velocity (Lorenz, 2007).

It is considered that the bombs composed of juvenile material were produced from a melted lava reservoir in the crater, whereas the faceted non-juvenile blocks were associated to crater-wall collapse or by ballistic ejection of early consolidated basaltic rocks. The more vesiculated interior of bombs is due to rapid chilling of the external surface of bombs after their emission from the vent in a plastic state. As the interior of bombs were still capable of plastic deformation, vesicle-rich zones were concentrated in the inner part of the bombs (Miyabuchi *et al.*, 2006).

DISCUSSION

The Sarmiento Formation is dominated by the deposition and reworking of fine ash strata in a continen-

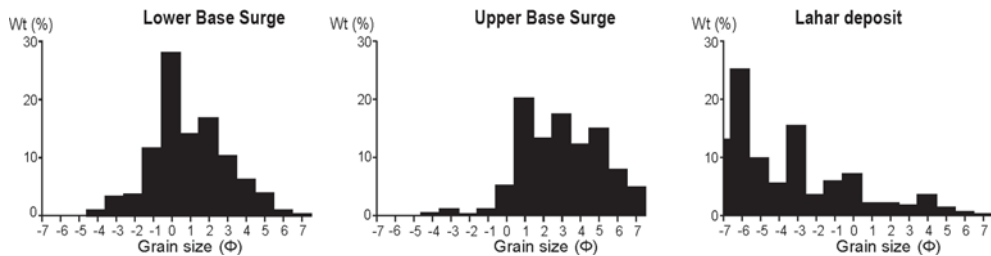


Figure 10. Grain size distribution of the lahar and base-surge deposits. Base-surge deposits show bimodal or polymodal distributions with maximum clast sizes at -4ϕ . Lahar deposits have polymodal distribution with main proportion of clasts at larger grain sizes.

Figura 10. Distribución de tamaño de grano de los depósitos de lahar y oleadas piroclásticas. Los depósitos de oleadas piroclásticas muestran distribución bimodal o polimodal con tamaños máximos de clasto de -4ϕ . Los depósitos de lahar tienen distribución polimodal, con la proporción principal de clastos en granulometrías mayores.

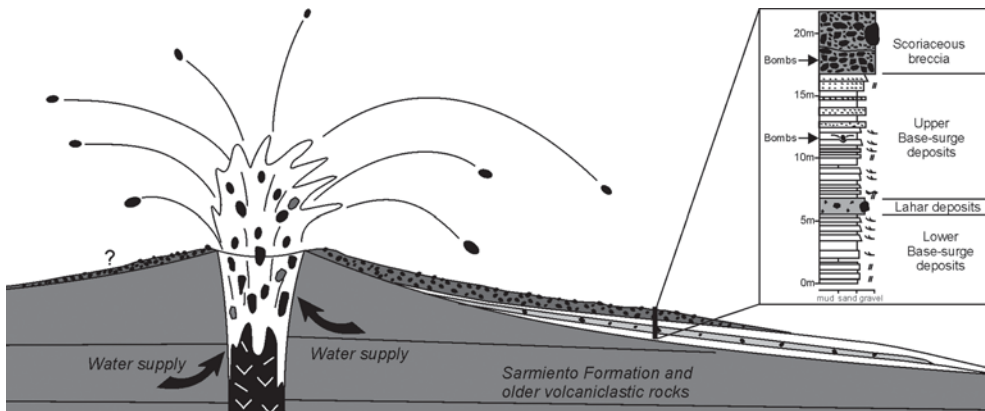


Figure 11. Inferred volcanic scenario for the analyzed volcaniclastic succession.

Figura 11. Escenario volcánico inferido para la sucesión volcanoclastica analizada.

tal, intracratonic setting, being the distal products of the magmatic activity of the Andean volcanic arc (Mazzoni, 1985). In the Golfo San Jorge Basin mafic alkaline volcanism occurs during the deposition of the Sarmiento Formation, mostly as subintrusive or hypabissal intrusions (*sensu* Walker, 1993). These bodies were emplaced at shallow depths and currently they are partially eroded, conforming hills of 50-200 m of relief over the adjacent topography (e.g., Cerro Negro, Cerro Dragón and Cerro Tortuga, among others). The presence of lava flows interbedded with ash-fall strata of the Sarmiento Formation is evidence that some of this bodies conformed pathways to the surface (Marshall *et al.*, 1977).

Vertical and lateral evolution of lithofacies associations in areas proximal to volcanic centers can be associated to eruptive conditions, i.e. the mixing ratio of water to magma, rate of magma supply and water-magma interactions at several scales (Sheridan and Wohletz,

1983; Head and Wilson, 1989). Most of the analyzed succession (lithofacies LF2, LF3, LF4, LF6) results from a relatively dry hydroclastic eruption, which produced the base surge lithofacies association composed mostly by coarse-grained particles and a minor fine component (Wohletz, 1983). Absence of ash beds containing accretionary lapilli also evidence lower steam content into the accompanying ash-cloud of the surges (Schumacher and Schmincke, 1991). Thin intercalations of finely laminated ash strata (lithofacies LF7) in the base surge evidence short-lived periods with efficient fragmentation of magma. The later lithofacies can indicate either a decrease in the rate of magma rise or an increase in the abundance of external water involved or both (Wohletz, 1986). In this scenario, the occurrence of poorly sorted, matrix supported deposits (lithofacies LF1) that conforms the lahar lithofacies association can be associated to a cohesive flow involving a significant proportion of interstitial water (magmatic or phreatic). The

scoriaceous breccia (lithofacies LF8) on top of the succession represents a magmatic (strombolian) eruption with little or no involvement of external water. The vertical occurrence of base surge and lahar lithofacies associations suggest variation in the proportion of available gas, steam (or water) of the system. Volcanic bombs falling in base surge deposits (lithofacies LF5) plus the occurrence of clast-supported, scoriaceous breccias (lithofacies LF8) interpreted as product of Strombolian-style eruptions on top indicates variable water-content and low-to-moderate volume flux, assuming gas content constant (Head and Wilson, 1989).

In spite of the lack of preservation of any volcanic edifice in the area, inferences could be made about the nature of the eruption from the lithofacies analysis, and a few inferences can be outlined about the type of crater, based on the features described in this contribution, regional considerations and comparisons with published models (e.g., Cas and Wright, 1987; Walker, 1993). The gas content, viscosity and yield strength of the basaltic magmas are rather uniform amongst different basaltic volcanoes, and diversity is mostly due to magma-supply rate and involvement of non-magmatic water. Basaltic eruptions with explosive character are frequently attributed to the interaction of ascending lavas with aquifers or phreatic water (Orton, 1996; Miyabuchi *et al.*, 2006). It is assumed that a lava lake or open conduit existed in the crater prior to the eruption, which provides molten material to the margins of the crater. The interaction of phreatic (or magmatic) water with magma should produce a violent explosion, providing the energy for rapid movement of the material in the flanks of the crater as a base surge and as bombs capable of plastic deformation. During periods of low rate of magma supply an strombolian-style eruption took place.

Several categories of volcanic edifice (maars, tuff rings and tuff cones) have been proposed, each with distinctive features (Cas and Wright, 1987). We should note that due to the lack of preservation of the volcanic edifice associated to the emplacement of the studied volcaniclastic succession, the following scenario is highly speculative. Maars are considered improbable for the generation of the studied volcaniclastic succession, due to the lack of preservation of the collapsed rim, lacustrine or aeolian lithofacies, and lack of accretionary lapilli. Tuff cones require steeper bedding angles (20-25°) than currently preserved. For this reason, the most probable scenario is the generation of a tuff ring above the intrusive rocks, with explosive interaction of magma with water close to or at the ground surface (Fig. 11).

CONCLUSIONS

Alkaline intrusives hosted in Cretaceous and Paleogene sedimentary rocks in the Golfo San Jorge Basin were emplaced in shallow depths, and some of them extruded lava flows over ash-fall beds of the Sarmiento Formation (middle Eocene to early Miocene). Near-vent volcaniclastic deposits exposed in the Cerro Dragón area evidence the development of a basaltic, hydrovolcanic explosive eruption. Eight volcaniclastic lithofacies are interpreted from this succession, which could be grouped into three lithofacies association: 1) volcaniclastic debris-flow (lahar), 2) base surge, and 3) scoriaceous breccias associated to a strombolian-style eruption. Well preserved plastic deformation of base surge deposits produced by ballistic fallout of several varieties of volcanic bombs evidence the explosive nature of the eruptions. Bombs are also preserved in the Strombolian stage of the eruption. These deposits are evidence of subaerial, explosive eruptions during the emplacement of the "PrePatagoniense" alkaline volcanism in Central Patagonia, whose constrictional craters are currently eroded.

Acknowledgements

The Facultad de Ciencias Naturales of the U.N.P.S.J.B. is thanked for logistic support. This research was founded by PI CIUNPAT N° 420 (U.N.P.S.J.B.), partially founded by the Ministerio de Educación y Ciencia (España) and the Grup de Qualitat of the Generalitat de Catalunya, España through Projects CGL2006-12415-C03-03 and SGR2005-00397 (DURSI). The authors would like to thanks Alberto Caselli, Corina Risso and the Editor, Gerardo Perillo, for constructive comments and suggestions that improved an earlier version of this article.

REFERENCES

- Ardolino, A., M. Franchi, M. Remesal y F. Salani**, 1999. La sedimentación y en volcanismo terciarios en la Patagonia extraandina. 2. El volcanismo en la Patagonia extraandina. In: R. Caminos (Ed.) *Geología Argentina*. Instituto de Geología y Recursos Minerales. Anales, 29:579-612. Buenos Aires.
- Arguden, A.T. and K.S. Rodolfo**, 1990. Sedimentologic and dynamic differences between hot and cold laharic debris flows of Mayon Volcano, Philippines. *Geological Society of America Bulletin* 102:865-876.
- Befus, K.S., R.E. Hanson, T.M. Lehman and W.R. Griffin**, 2008. Cretaceous basaltic phreatomagmatic volcanism in West Texas: Maar complex at Peña Mountain, Big Bend National Park. *Journal*

- of Volcanology and Geothermal Research* 73:245-264.
- Ayres, L.D., N.A. Van Wagoner and W.S. Ferreira**, 1991. Voluminous shallow-water to emergent phreatomagmatic basaltic volcaniclastic rocks, Proterozoic (~ 1886 ma) Amisk Lake Composite Volcano, Flin Flon Greenstone Belt, Canada. In: Fisher, R.V. and G.A. Smith (Eds). *Sedimentation in Volcanic Settings*. SEPM Special Publications, 45:175-187.
- Bellosi, E.S.**, 1990. Formación Chenque: Registro de la transgresión patagoniana en el Golfo San Jorge. *11º Congreso Geológico Argentino*, Actas 2:57-60. San Juan.
- Bellosi, E.S.**, 2005. Sedimentology and depositional setting of the Sarmiento formation (Eocene-Miocene) in central Patagonia. *16º Congreso Geológico Argentino*, Simposios: 306 (and extended version in CD format).
- Bellosi, E.S. y R.H. Madden**, 2005. Estratigrafía física preliminar de las secuencias piroclásticas terrestres de la formación Sarmiento (Eocene-Mioceno) en la Gran Barranca, Chubut. *16º Congreso Geológico Argentino*, Simposios: 305 (and extended version in CD format).
- Bellosi, E.S., M. Gonzalez, R. Kay y R. Madden**, 2002. El Valle inciso colhuehuapense de Patagonia Central (Mioceno inferior). *9º Reunión Argentina de Sedimentología*, Actas:49. Córdoba.
- Bitschene, P.R., R.E. Giacosa, and M. Márquez**, 1991. Geologic and mineralogical aspects of the Sarmiento Alkaline Province in Central Eastern Patagonia, Argentina. *6º Congreso Geológico Chileno*, Actas:328-331. Viña del Mar.
- Brady, L.F. and R.W. Webb**, 1943. Cored bombs from Arizona and California volcanic cones. *Journal of Geology* 51:398-410.
- Bull, S.W. and R.A.F. Cas**, 2000. Distinguishing base-surge deposits and volcaniclastic fluvial sediments: an ancient example from the Lower Devonian Snowy River Volcanics, south-eastern Australia. *Sedimentology* 47:87-98.
- Cas, R.A.F. and J.V. Wright**, 1987. *Volcanic Succession: Modern and Ancient*. Allen & Unwin. London.
- Chelotti, L.A., M.E. Vietto, R.J. Calegari y P.R. Bitschene**, 1996. Emplazamiento de cuerpos subvolcánicos de composición básica alcalina en el área Romberg - Wenceslao, cuenca Golfo San Jorge, Argentina. *13º Congreso Geológico Argentino* and *3º Congreso de Exploración de Hidrocarburos*, Actas 3:581-599. Buenos Aires.
- Clavijo, R.**, 1986. Estratigrafía del cretácico inferior en el sector occidental de la Cuenca Golfo San Jorge. *Boletín de Informaciones Petroleras*, 9:15-32. Buenos Aires.
- Cole, P.D., E. Fernandez, E. Duarte and A.M. Duncan**, 2005. Explosive activity and generation mechanisms of pyroclastic flows at Arenal volcano, Costa Rica between 1987 and 2001. *Bulletin of Volcanology* 67:695-716.
- Coussot, P. and M. Meunier**, 1996. Recognition, classification and mechanical description of debris flows. *Earth-Science Reviews* 40:209-227.
- Ferello, R.**, 1969. Intento de sistematización geocronológica de las rocas eruptivas básicas en sectores de Chubut y Santa Cruz. *4º Jornadas Geológicas Argentinas*, Actas 1:293-310. Buenos Aires.
- Feruglio, E.**, 1949. *Descripción Geológica de la Patagonia*, Yacimientos Petrolíferos Fiscales, Tomo 2:1-349. Buenos Aires.
- Feagle, J.G., T.M. Bown, C. Swisher and G. Buckley**, 1995. Age of the Pinturas and Santa Cruz Formation. *6º Congreso Argentino de Paleontología y Bioestratigrafía* Actas: 129-135. Trelew.
- Figari, E.G., M.S. Cid de la Paz and G. Laffitte**, 1996. Neocomian halfgrabens in the western San Jorge basin, Argentina: Petroleum System, Origin and Tectonic Inversion. II AAPG/SVG International Congress and Exhibition, Caracas, Venezuela. *American Association of Petroleum Geologists Bulletin* 80:1289-1290.
- Figari, E., E. Strelkov, G. Laffitte, M. S. Cid De La Paz, S. Courtade, J. Celaya, A. Vottero, P. Lafourcade, R. Martinez y H. Villar**, 1999. Los sistemas petroleros de la Cuenca del Golfo San Jorge: Síntesis estructural, estratigráfica y geoquímica. *4º Congreso de Exploración y Desarrollo de Hidrocarburos*, Actas: 197-237. Buenos Aires.
- Fisher, R.V.**, 1979. Models for pyroclastic surges and pyroclastic flows. *Journal of Volcanology and Geothermal Research* 13:339-371.
- Fisher, R.V. and H.U. Schmincke**, 1984. *Pyroclastic Rocks*. Springer-Verlag, Berlin.
- Foix, N., J.M. Paredes and R.E. Giacosa**, 2008. Paleo-earthquakes in passive-margin settings, an example from the Paleocene of the Golfo San Jorge Basin, Argentina. *Sedimentary Geology* 205:67-78.
- Francis, P.W.**, 1973. Cannonball bombs, a new kind of volcanic bomb from the Pacaya volcano, Guatemala. *Geological Society of America Bulletin* 84:2791-2794.
- Giacosa, R.E., J.M. Paredes, A. Nillni, M. Ledesma y F. Colombo**, 2004. Fallas normales de alto ángulo en el Neógeno del margen Atlántico de la Cuenca del Golfo San Jorge (46° S - 67° 30' O, Patagonia Argentina). *Boletín Geológico y Minero* 115:537-550.
- Hechem, J.J. y E.E. Strelkov**, 2002. Secuencia sedimentaria mesozoica del Golfo San Jorge. In: Haller, J.M. (Ed.) *Geología y Recursos Naturales de Santa Cruz*. Relatorio del 15º Congreso Geológico Argentino. Actas 1:129-147, Buenos Aires.
- Houghton, B.F., C.J.N. Wilson and I.E.M. Smith**, 1999. Shallow-seated controls on styles of explosive basaltic volcanism: a case study from New Zealand. *Journal of Volcanology and Geothermal Research* 91:97-120.
- Ingram, R.L.**, 1954. Terminology for the thickness of stratification and parting units in sedimentary rocks. *Geological Society of America Bulletin* 65:130-165.
- Head, J.W. and L. Wilson**, 1989. Basaltic pyroclastic eruptions: influence of gas-release patterns and volume fluxes on fountain structure, and the formation of cinder cones, rootless flows, lava ponds and lava flows. *Journal of Volcanology and Geothermal Research* 37:261-271.
- Kokelaar, B.P.**, 1986. Magma-water interactions in subaqueous and emergent basaltic volcanism. *Bulletin of Volcanology* 48:275-290.
- Legarreta, L., M. Uliana y M. Torres**, 1990. Secuencias deposicionales Cenozoicas de Patagonia Central: sus relaciones con las asociaciones de mamíferos terrestres y episodios marinos epicontinentales. *3º Simposio del Terciario de Chile*, Actas:135-176. Concepción.
- Legarreta, L., y M. Uliana**, 1994. Asociaciones de fósiles y hiatos en el Supracretácico-Neógeno de Patagonia: una perspectiva estratigráfico-secuencial. *Ameghiniana* 31:257-281.
- Lesta, P. y R. Ferello**, 1972. Región Extra-andina del Chubut y norte de Santa Cruz. In: Leanza, A.F. (Ed.) *Geología Regional Argentina*. Academia Nacional de Ciencias: 601-654. Córdoba.
- Lesta PJ., R. Ferello y G. Chebli**, 1980. Chubut extraandino. In: Turner, J.C.M. (Ed.) *Segundo Simposio de Geología Regional Argentina*. Academia Nacional de Ciencias, 2:1307-1387. Córdoba.
- Lorenz, V.**, 2007. Syn- and posteruptive hazards of maar-diatreme volcanoes. *Journal of Volcanology and Geothermal Research* 159:285-312.
- Lowe, D.R.**, 1982. Sediment gravity flows: II. Depositional models with special reference to the deposits of high density turbidity currents. *Journal of Sedimentary Petrology* 52:279-297.
- Macdonald, G.A.**, 1972. *Volcanoes*. Prentice-Hall, Englewood Cliffs, New Jersey.
- Marshall, L.G., R. Pascual, G.H. Curtis and R.E. Drake**, 1977.

- South American geochronology: radiometric time-scale for Middle to Late Tertiary mammal-bearing in Patagonia. *Science* 195:1325-1328.
- Marshall, L.G. y R. Pascual**, 1978. Una escala temporal radiométrica preliminar de las Edades Mamífero del Cenozoico medio y tardío Sudamericano. *Obra del Centenario del Museo de la Plata*, 5:11-28.
- Marshall, L.G., R.L. Cifelli, R.E. Drake and G.H. Curtis**, 1981. Calibration of the beginning of the age of Mammals in Patagonia. *Science* 204:43-45.
- Marshall, L.G., R.L. Cifelli, R.E. Drake and G.H. Curtis**, 1986. Vertebrate paleontology, geology, and geochronology of the Tapera de Lopez and Scarritt Pocket, Chubut Province, Argentina. *Journal of Paleontology* 60:920-951.
- Martin, U. and K. Németh**, 2006. How Strombolian is a «Strombolian» scoria cone? Some irregularities in scoria cone architecture from the Transmexican Volcanic Belt, near Volcán Ceboruco, (Mexico) and Al Haruj (Libya). *Journal of Volcanology and Geothermal Research* 155:104-118.
- Mazzoni, M.M.**, 1985. La Formación Sarmiento y el vulcanismo paleógeno. *Revista Asociación Geológica Argentina* 40:60-68.
- Mazzoni, M.M.**, 1994. Conos de cinder y facies volcanoclásticas miocenas en la Meseta de Canquel (Scarritt Pocket), provincia de Chubut, Argentina. *Revista Asociación Argentina de Sedimentología* 1:15-31.
- Miyabuchi, Y., K. Watanabe and Y. Egawa**, 2006. Bomb-rich basaltic pyroclastic flow deposits from Nakadake, Aso Volcano, southwestern Japan. *Journal of Volcanology and Geothermal Research* 155:90-103.
- Németh, K. and J.D.L. White**, 2003. Reconstructing eruption processes of a Miocene monogenetic volcanic field from vent remnants: Waipati Volcanic Field, South Island, New Zealand. *Journal of Volcanology and Geothermal Research* 124:1-21.
- Németh, K., U. Martin, and S. Harangi**, 2001. Miocene phreatomagmatic volcanism at Tihany (Pannonian Basin, Hungary). *Journal of Volcanology and Geothermal Research* 111:111-135.
- Orton, G.J.**, 1996. Volcanic Environments. In: Reading H.G. (Ed.) *Sedimentary Environments: Processes, Facies and Stratigraphy* (3rd Ed.), Blackwell, Oxford, pp. 485-567.
- Panza, J.L. and M.R. Franchi**, 2002. Magmatismo basáltico Cenozoico Extrandino. In: Haller, M.J. (Ed.) *Geología y Recursos Naturales de Santa Cruz*. Relatorio del 15º Congreso Geológico Argentino. I-14:201-236. El Calafate.
- Parfitt, E.A.**, 2004. A discussion of the mechanism of explosive basaltic eruptions. *Journal of Volcanology and Geothermal Research* 134:77-107.
- Pascual R. y O. Odreman Rivas**, 1973. Las unidades estratigráficas del Terciario portadoras de mamíferos. Su distribución y sus relaciones con los acontecimientos distróficos. *5º Congreso Geológico Argentino*, 3:293-338.
- Pettijohn, F.J. and P.E. Potter**, 1964. *Atlas and Glossary of Primary Sedimentary Structures*. Springer-Verlag, New York.
- Postma, G.**, 1986. Classification of sediment gravity flow deposits based on flow conditions during sedimentation. *Geology* 14:291-294.
- Risso, C., K. Németh, A.M. Combina, F. Nullo and Drosina, M.**, 2008. The role of phreatomagmatism in a Plio-Pleistocene high-density scoria cone field: Llancanelo Volcanic Field (Mendoza), Argentina. *Journal of Volcanology and Geothermal Research* 169: 61-86.
- Rodriguez, J.F.R and R. Littke**, 2001. Petroleum generation and accumulation in the Golfo San Jorge Basin, Argentina: a Basin modeling study. *Marine and Petroleum Geology* 18:995-1028.
- Schumacher, R. and H.U. Schmincke**, 1991. Internal structure and occurrence of accretionary lapilli – a case study at Laacher See Volcano. *Bulletin of Volcanology* 53:612-634.
- Sciutto, J.C., O. Cesari and N. Iantinos**, 2000. Hoja Geológica 4569-IV, Escalante (Provincia del Chubut). Instituto de Geología y Recursos Minerales, Servicio Geológico Minero Argentino. Boletín Inédito (Buenos Aires).
- Sheridan, M.F. and K.H. Wohletz**, 1983. Hydrovolcanism: basic considerations and review. *Journal of Volcanology and Geothermal Research* 17:1-29.
- Simpson, G.G.**, 1940. Review of the mammal-bearing Tertiary of South America. *Proceedings of the American Philosophy Society* 83:649-709.
- Simpson, G.G.**, 1941. The Scarrit expeditions of the American Museum of Natural History, 1930-1934. *Science* 80:207-208.
- Smith G.A.**, 1987. The influence of explosive volcanism on fluvial sedimentation: The Deschutes Formation (Neogene) in central Oregon. *Journal of Sedimentary Petrology* 57:613-629.
- Sohn, Y.K. and S.K. Chough**, 1989. Depositional processes of the Suwolbong tuff ring, Cheju Island (Korea). *Sedimentology* 36:837-855.
- Spadaro, F.R., R.A. Lefèvre and P. Auseet**, 2002. Experimental rapid alteration of basaltic glass: implications for the origins of atmospheric particulates. *Geology* 30:671-674.
- Spalletti, L.A. y M.M. Mazzoni**, 1977. Sedimentología del Grupo Sarmiento en un perfil ubicado al sudeste del Lago Colhué Huapi, provincia del Chubut. *Obra del Centenario del Museo de la Plata* 4:261-283.
- Spalletti, L.A. y M.M. Mazzoni**, 1979. Estratigrafía de la Formación Sarmiento en la barranca Sur del Lago Colhué Huapi, Provincia del Chubut. *Revista Asociación Geológica Argentina* 34:271-281.
- Vazquez, J.A. and M.H. Ort**, 2006. Facies variation of eruption units produced by the pasaje of single pyroclastic surge currents, Hopi Buttes volcanic field, USA. *Journal of Volcanology and Geothermal Research* 154:222-236.
- Vesperman, D. and H.U. Schmincke**, 2000. Scoria cones and tuff rings. In: Sigurdsson, H. (Ed.), *Encyclopedia of Volcanoes*. Academic Press, San Diego, pp. 683-694.
- Vietto, M.E. y P.R. Bitschene**, 1994. Geología, petrología y estilo de emplazamiento de basaltos alcalinos en el borde sur de la cuenca del Golfo San Jorge (Patagonia Central, Argentina). *Zentralblatt für Geologie u. Paläontologie, Teil I*, (7/8):739-752. Stuttgart.
- Walker, G.P.L.**, 1984. Characteristics of dune-bedded pyroclastic surge bedsets. *Journal of Volcanology and Geothermal Research* 20:281-296.
- Walker, G.P.L.**, 1993. Basaltic-volcano systems. In: Prichard, H.M., T. Alabaster, N. Harris, and C.R. Neary (Eds.) *Magmatic Processes and Plate Tectonics*. Geological Society Special Publication 76:3-38.
- White, J.D.L.**, 1991. The depositional record of small, monogenetic volcanoes within terrestrial basins. In: Fisher, R.V. and G.A. Smith (Eds.). *Sedimentation in Volcanic Settings*. SEPM Special Publications, 45:155-171.
- Wohletz, K.H.**, 1983. Mechanisms of hydrovolcanic pyroclast formation: Grain-size, scanning electron microscopy, and experimental data. *Journal of Volcanology and Geothermal Research* 17:31-64.
- Wohletz, K.H.**, 1986. Explosive magma-water interactions: thermodynamics, explosion mechanics, and field studies. *Bulletin of Volcanology* 48:245-264.